1521-009X/47/10/1156–1163$35.00
DRUG METABOLISM AND DISPOSITION

https://doi.org/10.1124/dmd.118.086132
Drug Metab Dispos 47:1156–1163, October 2019

Special Section on Pharmacokinetic and Drug Metabolism Properties of Novel Therapeutic Modalities

Catalytic Cleavage of Disulfide Bonds in Small Molecules and Linkers of Antibody–Drug Conjugates[S]

Donglu Zhang, Aimee Fourie-O'Donohue, Peter S. Dragovich, Thomas H. Pillow, Jack D. Sadowsky, Katherine R. Kozak, Robert T. Cass, Liling Liu, Yuzhong Deng, Yichin Liu, Cornelis E.C.A. Hop, and S. Cyrus Khojasteh

Drug Metabolism & Pharmacokinetics (D.Z., R.T.C., L.L., Y.D., C.E.C.A.H., S.C.K.), Biochemical and Cellular Pharmacology (A.F.-O., K.R.K., Y.L.), Discovery Chemistry (P.S.D., T.H.P.), and Protein Chemistry (J.D.S.), Genentech, Inc., South San Francisco, California

Received December 24, 2018; accepted May 7, 2019

ABSTRACT

In cells, catalytic disulfide cleavage is an essential mechanism in protein folding and synthesis. However, detailed enzymatic catalytic mechanism relating cleavage of disulfide bonds in xenobiotics is not well understood. This study reports an enzymatic mechanism of cleavage of disulfide bonds in xenobiotic small molecules and antibody conjugate (ADC) linkers. The chemically stable disulfide bonds in substituted disulfide-containing pyrrolobenzodiazepine (PBD, pyrrolo[2,1-c][1,4]benzodiazepine) monomer prodrugs in presence of glutathione or cysteine were found to be unstable in incubations in whole blood of humans and rats. It was shown the enzymes involved were thioredoxin (TRX) and glutaredoxin (GRX). For a diverse set of drug-linker conjugates, we determined that TRX in the presence of TRX-reductase and NADPH generated the cleaved products that are consistent with catalytic disulfide cleavage and linker immolation. GRX was less rigorously studied; in the set of compounds studied, its role in the catalytic cleavage was also confirmed. Collectively, these in vitro experiments demonstrate that TRX as well as GRX can catalyze the cleavage of disulfide bonds in both small molecules and linkers of ADCs.

Introduction

The disulfide bond (C-S-S-C) is a common structural motif in proteins. Disulfides have been used recently as targeted drug-delivery approaches (prodrugs) (Vrudhula et al., 2002; Chen and Hu, 2009; Zhang et al., 2017b), which use the higher levels of reducing agent glutathione (GSH) to selectively release various cytotoxic agents in tumors (Gamcsik et al., 2012; Hatem et al., 2017). Pillow et al. (2017a,b) reported a self-immolating disulfide linker (β-mercaptoethyl-carbamate, $-SCH_2CH_2OCO^-$) that can be directly attached to cysteine thiols of antibodies where the cysteine residues are engineered into antibody light or heavy chains (called THIOMAB antibodies) (Zhang et al., 2016). The cleavage of disulfide linker was proposed to occur through GSH or cysteine reductive cleavage of the cysteine-thiolate intermediate after conjugate internalization and lysosomal proteolysis. In this mechanism, payload was released after linker immolation following chemical cleavage of the disulfide bond (Zhang et al., 2016; Pillow et al., 2017a,b). Disulfide bond linkers have also been used in other antibody conjugates (Erickson et al., 2010; Kellogg et al., 2011), chemosensors (Lee et al., 2013), and nanoparticles (Wang et al., 2014; Zhang et al., 2017a).

Pyrrolo[2,1-c][1,4]benzodiazepine (PBD monomer 1) and its dimer (PBD dimer 2) belong to a class of DNA alkylators that covalently modify DNA minor grooves (Hartley, 2011). Recently, several antibody drug conjugates (ADCs) using PBD analogs as drugs have entered clinical trials (Jeffrey et al., 2013; Saunders et al., 2015). In the process of developing the next generation of ADCs, we sought to design an ADC with a disulfide-containing linker and the prodrug of a cytotoxic payload that could be selectively activated by the high reducing potential present in many intratumor environments after targeted antibody-mediated delivery (Pei et al., 2018).

Disulfide bonds between cysteines are an integral part of protein structures, and these disulfide bonds were formed during protein synthesis, folding, and posttranslational modifications. Thioredoxin (TRX) TRX and glutaredoxin (GRX) are the specific enzymes catalyzing cleavage of the disulfide bonds that were formed between a cysteine residue and glutathione that was used initially to protect newly incorporated cysteine residues or between cysteine residues for posttranslational modifications (Hogg, 2003, 2009; Chen and Hogg, 2006; Azimi et al., 2011). TRX and GRX are cytosolic enzymes of 10–12 kDa in size. TRX could be located outside cells, cytoplasm,

https://doi.org/10.1124/dmd.118.086132.
[S]This article has supplemental material available at dmd.aspetjournals.org.

ABBREVIATIONS: ADC, antibody drug conjugate; DAR, drug to antibody ratio; GRX, glutaredoxin; GSH, glutathione; HBS-EP buffer, 0.01 M HEPES pH 7.4, 0.15 M NaCl, 3 mM EDTA, 0.005% v/v Surfactant P20; LC-MS, liquid chromatography with mass spectrometry; LC-MS/MS, liquid chromatography with tandem mass spectrometry; PBD, pyrrolo[2,1-c][1,4]benzodiazepine; SA, streptavidin-coated; TRX, thioredoxin.

nucleus, or mitochondria with a cellular concentration of 2–12 μM and plasma concentration of up to 6 nM. TRX reductase and NADPH are required for TRX catalytic activity (Holmgren and Bjornstedt, 1995; Mustacich and Powis, 2000). GRX concentration in red blood cells could be at 1 μM with an optimal pH 8.0 for catalytic activity. GRX also requires a reductase and NADPH or GSH as a cofactor. In this study, recombinant enzymes TRX and GRX demonstrated catalytic activities for cleavage of disulfide bonds in xenobiotics. The catalytic activities of disulfide cleavage in whole blood are consistent with the activities of TRX and GRX although low cofactor concentrations in blood may have limited their optimal catalytic activities toward xenobiotic disulfides.

During the process of selecting disulfides through stability testing in buffer in the presence of GSH or cysteine and whole blood, distinct stability profiles were observed for disulfides with less substitution at the adjacent carbons. These results suggested a biologic mechanism that catalyzes certain disulfide cleavages. Subsequently, we conducted experiments to investigate the potential catalytic activity of TRX and GRX, two common oxidoreductase enzymes that are present in whole blood (Björnstedt et al., 1995; Holmgren and Bjornstedt, 1995; Butera et al., 2014; Pei et al., 2018). Incubation of small molecule disulfide compounds with TRX produced expected products. Incubation of these enzymes with the disulfide-linker ADC also produced the expected payload, compound 2. In addition, incubation of an ADC containing both a disulfide prodrug and a disulfide-linker produced several products that are consistent with cleavage of either disulfide bonds. These results suggested that TRX and GRX can catalyze cleavage of disulfide bonds in small molecules as well as in the linker of an ADC.

Materials and Methods

Materials. Ammonium formate, formic acid, NADPH, human recombinant human thioredoxin, rat liver thioredoxin reductase, and proprietary thioredoxin reductase inhibitor (catalog no. T9199) were purchased from Sigma-Aldrich (St. Louis, MO). Human glutaredoxin I, rat recombinant TRX, and glutaredoxin reductase were purchased from Creative Biomart (Shirley, NY) (Fig. 1). Compounds 1–10 were made as described elsewhere (Pei, et al., 2018). Synthesis of compounds 11 and B8 are described in the Supplemental Information section. Conjugate 12 was prepared as described elsewhere. Human CD22 antibodies with two engineered cysteine residues were generated as described elsewhere (Bhakta et al., 2013; Junutula and Gerber, 2016; Ohri et al., 2018). The ADC conjugate 13 was synthesized from the linker drug B8 as described elsewhere (Staben et al., 2016; Zhang et al., 2016). The antibody to drug ratio was 1.9 and 2.0, respectively for ADCs 12 and 13.

In Vitro Incubations in Buffer or with Enzymes. The compounds were incubated at 10 μM with 0.03 and 0.2 mM cysteine or 4 mM GSH, in 100 mM Tris buffer, pH 7.0, containing 5% methanol at 37°C. Aliquots were taken at 0, 1, 4, and 24 hours, and the samples were analyzed by liquid chromatography with tandem mass spectrometry (LC-MS/MS).

Selected disulfide prodrugs 3, 5, and 10) at 10 μM and ADC 12 and 13 at 1.6 μM (0.25 mg/ml) were separately incubated with human or rat recombinant TRX at 100 nM (1 μg/ml) with TRX reductase 20 nM and NADPH (5 mM) or human recombinant GRX at 100 nM (1.2 μg/ml) and 80 μM GSH in 100 μl of Tris buffer (100 mM, pH 7.4) incubation for 1 and 2 hours at 37°C with water bath shaking at 120 rpm. Control incubations without NADPH or GSH were also included. In addition, the proprietary TRX reductase inhibitor at 1 mM was used in some of incubations. Acetonitrile (0.2 ml) was added to quench the reactions. After centrifugation, aliquots of 10 μl were injected for liquid chromatography with mass spectrometry (LC-MS) analysis using the condition described in next section.

LC-MS Analysis for Identification of Small Molecular Catabolites. The samples from in vitro incubations of buffer, enzymes, or whole blood were done on Sciex TripleTOF 5600 on a Hypersil Gold C18 column (100 × 2.1, 1.9 μM; Thermo Scientific). The column was eluted by a gradient of buffer A (0.1% formic acid in 10 mM ammonium acetate) to buffer B (0.1% formic acid in 10 mM ammonium acetate in 90% acetonitrile), 5% B at 0–0.5 minutes, 5%–25% B at 0.5–8 minutes, 25%–75% B at 8–13 minutes, and 75%–95% B at 13–13.5 minutes; 95% B at 13.5–14.5 minutes, and 95%–5% B at 14.5–15 minutes at 0.4 ml/min. All products were separated and characterized by LC-MS/MS in a positive electrospray ionization mode. All analytes had the protonated molecular ($[MH]^+$) as the major species with little source fragmentation. Full scan accurate mass peak areas were used to estimate relative abundance of each species. The disappearance of starting material estimated based on relative full scan peak areas was consistent with that estimated based on the relative abundance compared with time 0 by MS or UV (200–350 nm). The disulfide cleavage versus time profiles were obtained, and the percentage of parent remaining at individual time points was reported.

The identification of compounds was done by LC-MS on a Triple TOF 5600 mass spectrometer (AB Sciex) coupled with high-pressure liquid chromatography

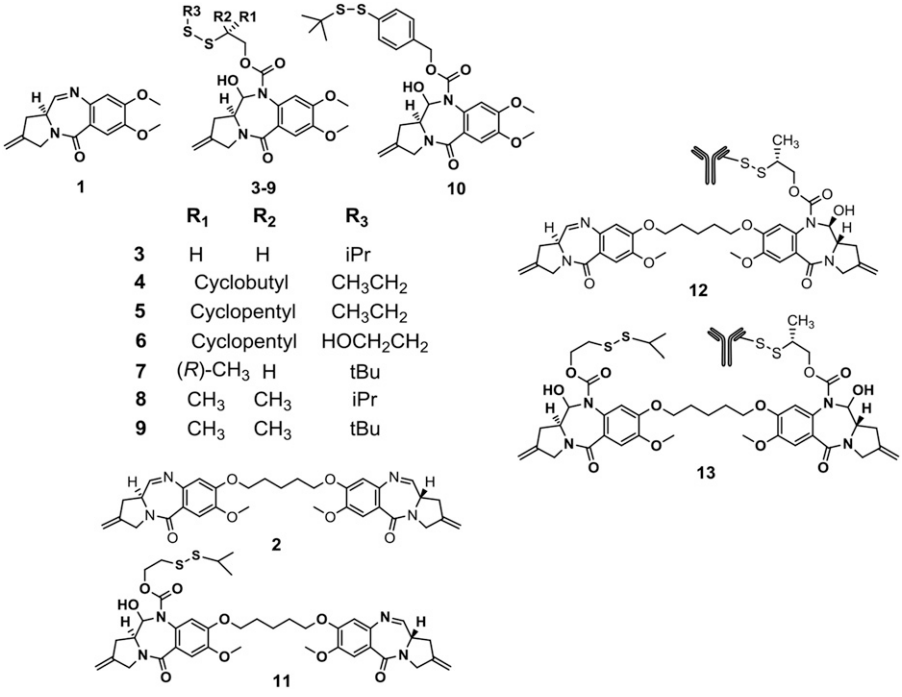

Fig. 1. Chemical structures of disulfide-containing prodrugs and ADC conjugates studies.

TABLE 1

Stability difference of disulfide-containing prodrugs in incubations with GSH, cysteine, or human and rat whole blood

Compound	% Disulfide Remaining			
	GSH, 4.0 mM[a]	Cysteine, 30 μM[a]	Rat Whole Blood[b]	Human Whole Blood[b]
3	56	100	0.1	5
4	21	99	0.3	24
5	68	100	5	80
6	44	98	1	45
7	88	100	87	120
8	100	100	19	120
9	100	100	100	108
10	82	99	124	124

[a]Disulfide cleavage in presence of indicated concentration of GSH or cysteine at 24 hours. See the Supplemental Information for additional details.

[b]Disulfide was incubated with whole blood, and aliquots were analyzed at 24 hours. Procaine (10 μM) was used as the positive-control incubation with <3% remaining after 24 hours.

separation. PBD-dimer 2 was identified by the molecular ion at *m/z* found: 585.2730 and calculated: 585.2713, $C_{33}H_{37}N_4O_6$ and by major fragments at *m/z*: 504.2144 and 259.1096. Compound 11 was identified by molecular ion at *m/z* found: 781.2968 and calculated: 781.2941, $C_{39}H_{49}N_4O_9S_2$ and by major fragments at *m/z*: 719.2991. Compound 16 was identified by molecular ion at *m/z* found: 841.2889 and calculated: 841.2788, $C_{40}H_{49}N_4O_{12}S_2$ and by major fragments at *m/z*: 823.2696, 705.2538, 608.2086, and 535.1915. Other compounds were identified from comparison with synthetic materials.

Whole Blood Stability. Human and rat blood (100 μl of pool of mixed gender) was incubated with 10 μM of a compound (1–10) at 37°C for 0, 4 and 24 hours ($n = 3$). Acetonitrile (300 μl) was used to quench the reaction. After vortexing and sonication for 5 minutes, the samples were centrifuged for 10 minutes at 2000*g*. The supernatant (50 μl) was mixed with 200 μl of water, and 10 μl was analyzed by LC-MS/MS. The GSH analysis was performed with a Shimadzu Nexera UPLC system coupled to a QTRAP 5500 AB Sciex in positive ion mode. Mobile phase A was water, and B was acetonitrile, both with 0.1% formic acid. The chromatography was performed on a Thermo HyperCard column 50 × 2.1 mm, 3 μm (Bellefonte, PA). Propranolol (100 nM) was used as internal standard. The calibration curve for quantitation of a compound was constructed by plotting the compound to internal standard peak area ratio versus the nominal concentration of the analyte with a weighted 1/x quadratic regression.

For incubation of ADC conjugates in whole blood, whole blood was shipped overnight cold by the vendor (Bioreclamation, Westbury, NY), and stability samples were created immediately upon arrival. Initial dilutions of the ADC source material were made in buffer (1× PBS, pH 7.4, 0.5% bovine serum albumin, 15 ppm Proclin) so that all molecules were 1 mg/ml in concentration. Then a 1:10 dilution (36 μl of 1 mg/ml initial dilution + 324 μl blood or buffer) was performed to generate the stability samples with a final concentration of 100 μg/ml. Once mixed, 150 μl of the whole blood/buffer stability samples were aliquoted into two separate sets of tubes for the two different time points (0 and

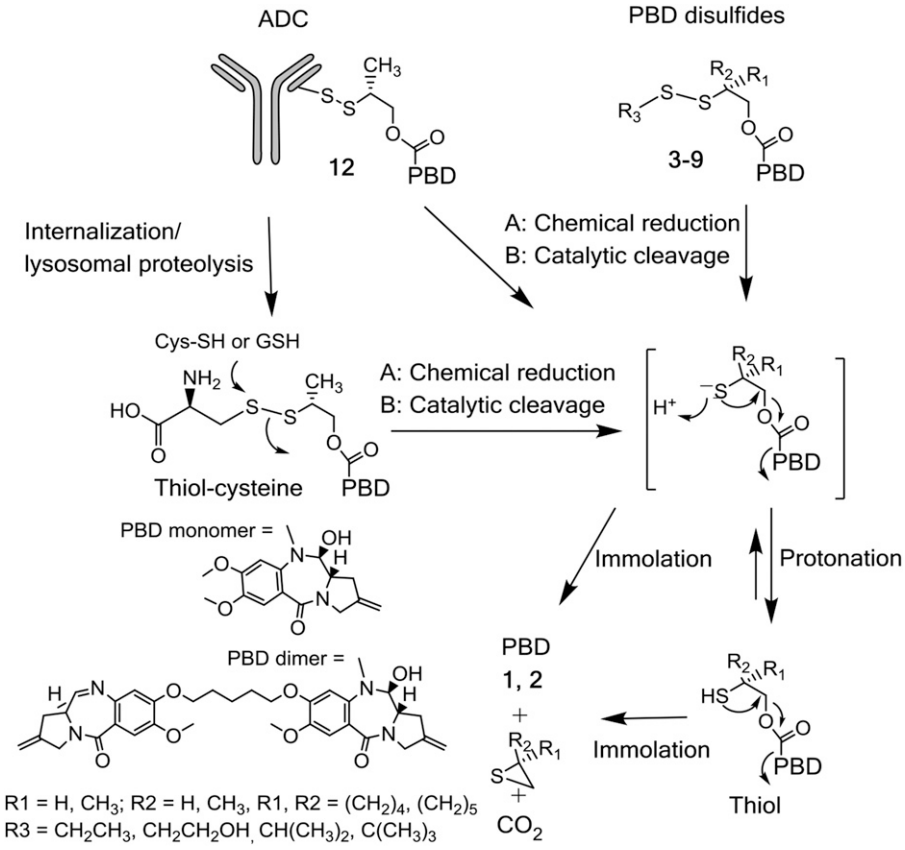

Fig. 2. Chemical (A) and catalytic (B) disulfide cleavage mechanisms for disulfide-containing prodrugs and disulfide linker-containing ADCs.

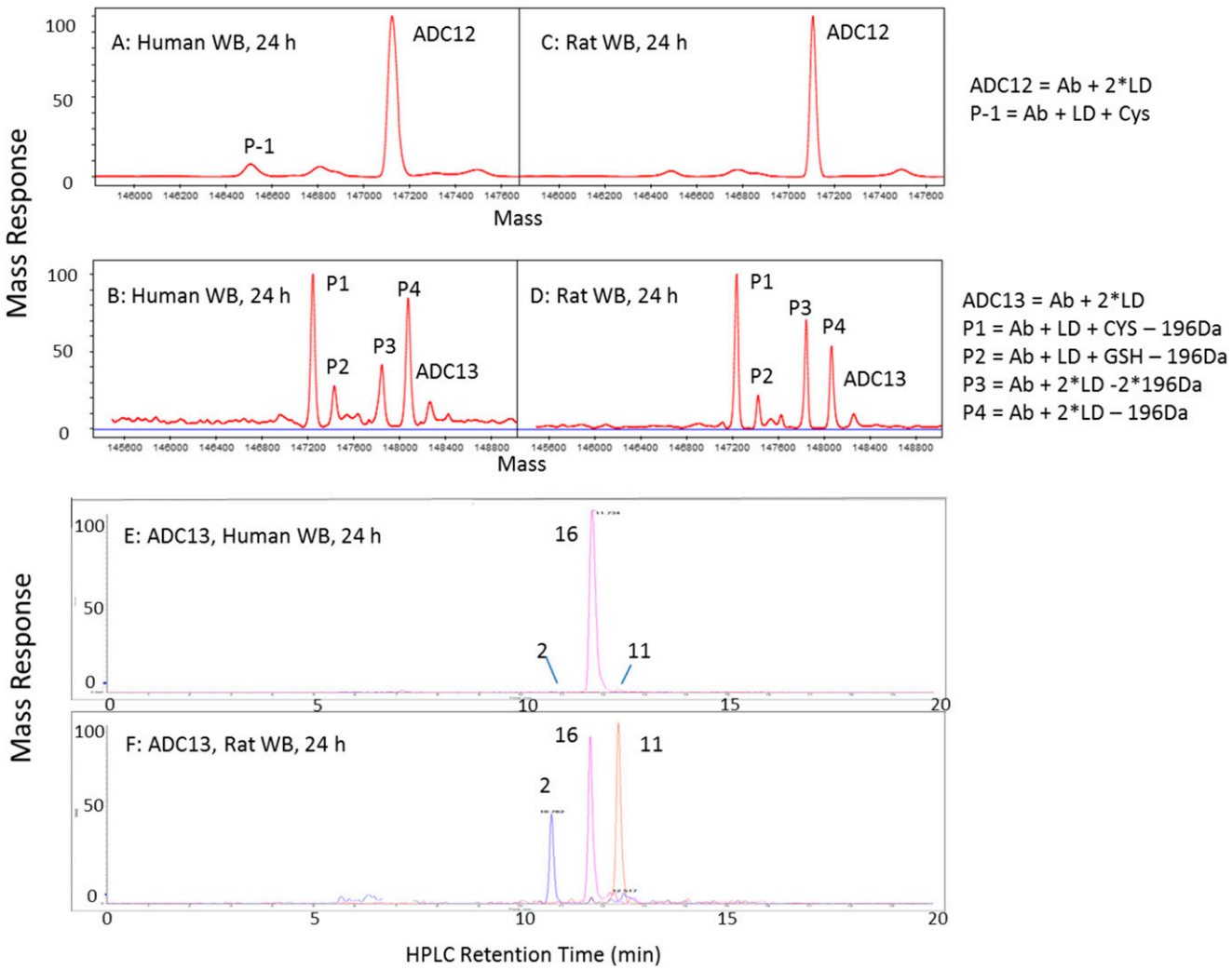

Fig. 3. Degradation product profile of ADC 13 from human and rat blood incubations.

24 hours). The 0-hour samples were placed in a −80°C freezer, and the 24-hour samples were placed in a 37°C incubator and shaken (~700 rpm). After 24 hours, the samples were removed from the incubator and stored in a −80°C freezer until LC-MS was performed. The matrices used to generate the samples were mouse (CB17 SCID), rat (Sprague-Dawley), and human.

Whole blood stability samples were analyzed by affinity-capture LC-MS with modifications to the method described elsewhere (Su et al., 2016). Briefly, streptavidin-coated (SA) magnetic beads (Thermo Fisher Scientific, Waltham, MA) were washed 2 times with HBS-EP buffer (0.01 M HEPES pH 7.4, 0.15 M NaCl, 3 mM EDTA, 0.005% v/v Surfactant P20; GE Healthcare, Sunnyvale, CA), then mixed with either biotinylated extracellular domain of target (e.g., human erb2) or anti-idiotypic antibody for specific capture using a KingFisher Flex (Thermo Fisher Scientific) and incubated for 2 hours at room temperature with gentle agitation. After the 2 hours, the SA-bead/biotin-capture probe complex was washed 2 times with HBS-EP buffer, mixed with stability samples that were diluted 1:16 with HBS-EP buffer, then incubated for 2 hours at room temperature with gentle agitation. After the 2 hours, the SA-bead/biotin-capture probe/sample complex was washed 2 times with HBS-EP buffer followed by deglycosylation overnight with PNGase F (New England BioLabs, Ipswich, MA). The SA-bead/biotin-capture probe/sample complex was then washed 2 times with HBS-EP buffer, followed by two washes with water (Optima H2O; Fisher Scientific, Pittsburgh, PA) and finally one wash with 10% acetonitrile. The beads were then placed in 30% acetonitrile/0.1% formic acid for elution where they were incubated for 30 minutes at room temperature with gentle agitation before being collected. The eluted samples were then loaded on to the LC-MS (Synapt-G2S; Waters, Milford, MA) for analysis.

ADC samples (10 μl) were injected and loaded onto a PepSwift reversed phase monolithic column (500 μm × 5 cm; Thermo Fisher Scientific) maintained at 65°C using a Waters Acquity UPLC system at a flow rate of 20 μl/min with the following gradient: 20% B (100% acetonitrile + 0.1% formic acid) at 0–2 minutes; 35% B at 2.5 minutes; 65% B at 5 minutes; 95% B at 5.5 minutes; and 5% B at 6 minutes. The column was directly coupled for online detection with Waters Synapt G2-S Q-ToF mass spectrometry operated in positive electrospray ionization mode with an acquisition range from *m/z* 500 to 5000.

For stability data analysis, deconvolution of the raw spectrum within a selected ADC elution time window was implemented with Waters BiopharmaLynx 1.3.3 software. The drug loss or modifications were identified according to the corresponding mass shifts from the starting ADC material. Peak labeling and % DAR calculation was performed with a custom Vortex script (Dotmatics, Bishops Stortford, United Kingdom). The drug loss, cleavage, or adducts formation were identified according to the corresponding mass shifts from the starting ADC material. Relative abundance of each ADC species in the analytic sample was represented by its MS signal intensity. The relative ratios of ADC with different DARs were calculated by dividing the intensity of the specific ADC species with the intensity from the total ADC species. DAR percentage was calculated as previously reported elsewhere (Staben et al., 2016).

Results

The stability of disulfide bonds in substituted disulfide-containing PBD monomer prodrugs 3–10 were tested in the incubations with GSH

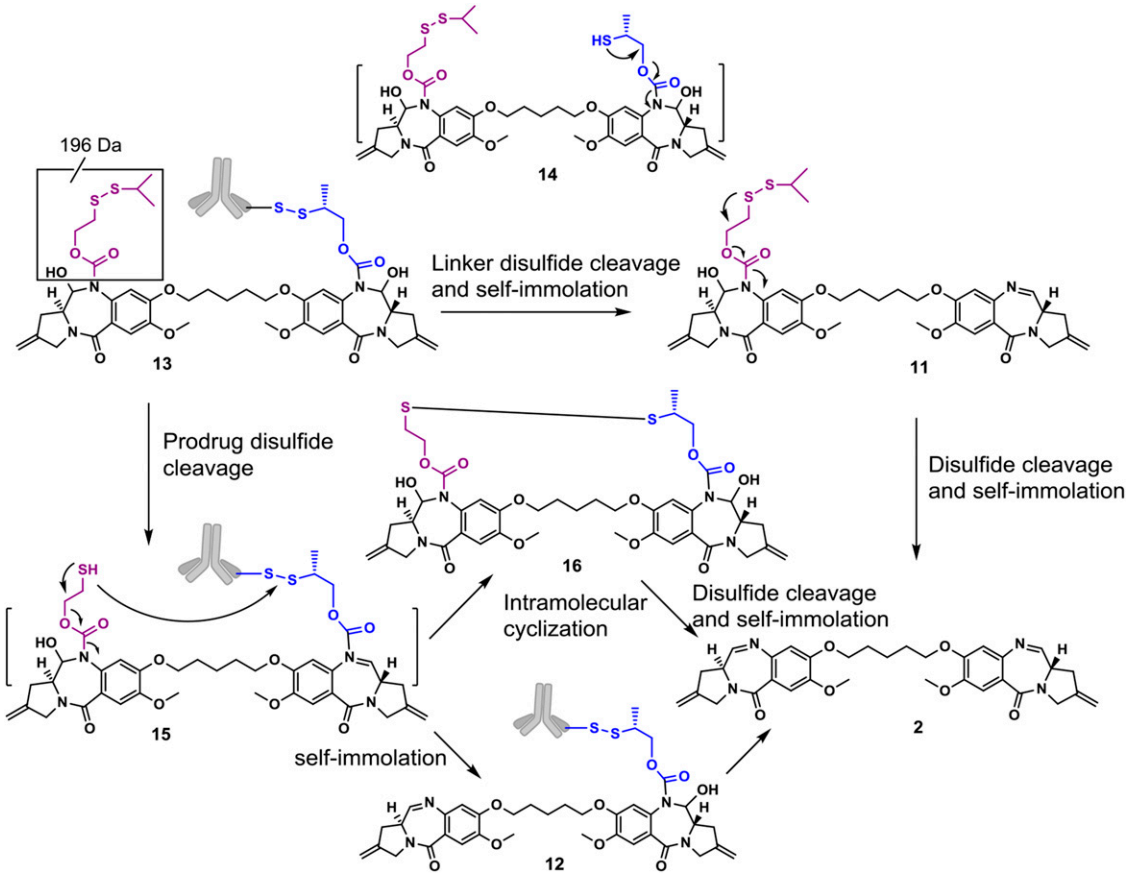

Fig. 4. Proposed payload-related product formation pathways of ADC 13 in incubation in human and rat blood.

and cysteine. Subsequently, some stable compounds that were selected from a glutathione/cysteine reduction assay were shown to be unstable in incubations in whole blood of humans and rats. Disulfides 3–6 which contained the disulfide prodrug functionality were relatively stable in incubations with 4 mM GSH or 30 μM cysteine up to 24 hours at 37°C (Table 1). However, these compounds were not stable in the incubations in whole blood of human or rat (Supplemental Fig. S1; Table 1), with far fewer percentage remaining of the starting material at the end of incubations.

In addition, more enzymatic cleavage was observed in rat blood compared with human blood. In comparison, disulfides 7–10, which have more substitutions on carbon atoms next the disulfide bond, showed better stability than the less substituted disulfides 3–6 in both GSH/cysteine reduction assays and whole blood incubations. The product from these whole blood incubations was the expected PBD monomer 1. Figure 2 (pathway A) showed that chemical reduction of the disulfide bond followed by immolation of the β-mercaptoethyl-carbamate linker produced PBD monomer 1.

To better understand the role of free thiols in degradation of these disulfide compounds in blood, we also determined the GSH and cysteine concentrations in whole blood and blood cells of rats and humans (Supplemental Table 1). The GSH and cysteine concentrations in the plasma of rats and humans were relatively low at single micromolar ranges. On the other hand, the GSH concentrations in blood cells can reach millimolar ranges while the cysteine concentration was at low micromolar ranges. These results are consistent with the values found in the literature (Sato et al., 2005; Johnson et al., 2008; Otani et al., 2011; Gamcsik et al., 2012; Hatem et al., 2017). In these in vitro incubations, the concentrations of the reductants were higher than those found in whole blood or blood cells of human or rat yet caused much less disulfide cleavage.

Figure 3, A and C, show the product profiles of ADC 12 from the 24-hour incubations in the whole blood of humans and rats. The disulfide linker containing ADC 12 showed relatively good stability; only low levels of deconjugation products (P-1) were observed in both human and rat blood samples after 24 hours of incubation at 37°C.

Probe ADC molecule 13 was designed to contain both a disulfide prodrug functionality and a disulfide linker on a PBD dimer 2. Compared with conjugate 12, which was relatively stable in whole blood incubation (Fig. 3, A and C), the prodrug ADC 13 was not stable in whole blood of humans or rats, with formation of multiple products that resulted from the loss of one or two prodrug functionalities (−196 Da) or the loss of one or two linker drugs (-LD) or a combination of these degrading processes.

Figure 3, B and D–F, shows the degradation profiles of ADC 13. Although antibody-related product profiles look similar between humans and rats, the payload-related product profile are very different. From incubation with human blood, the intramolecular disulfide 16 was the dominant product with payload 2 and prodrug 11 as minor products. In contrast, incubation in rat blood generated all three products (2, 11, 16) as prominent products. There was presumably a higher level of degradation activity in rat blood compared with human blood to further cleave 16 to 2.

Figure 4 shows the degradation pathway of ADC 13 in human and rat blood. In this pathway, linker disulfide cleavage resulted in formation of intermediate 14, which can quickly immolate to form 11. The disulfide cleavage in the prodrug functionality of ADC 13 would generate intermediate 15, which may immolate to form

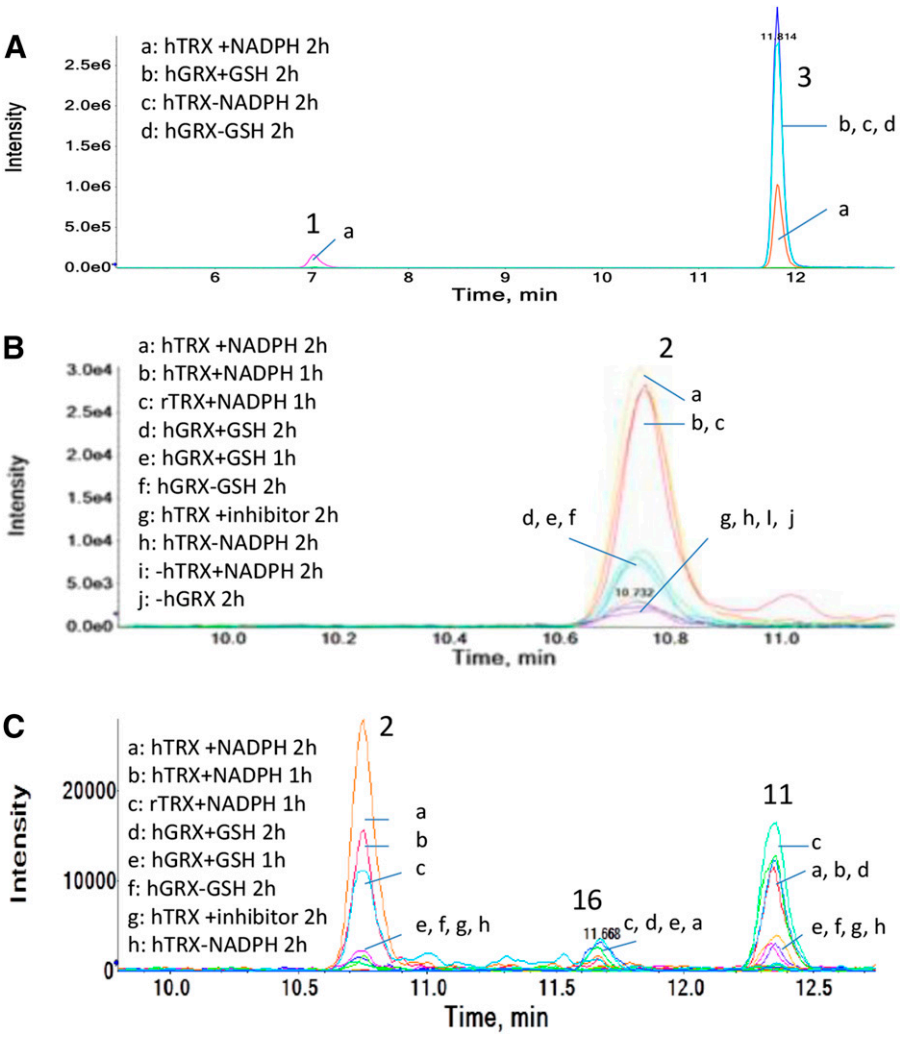

Fig. 5. PBD-related product profile of disulfide 3 (A), ADC 12 (B), and ADC 13 (C) in catalytic reactions by TRX and GRX.

conjugate 12 (which is also labeled as P3 in the chromatograms). Intermediate 15 could also lead to formation of 16 through the intramolecular disulfide formation. The immolation of the less substituted β-mercaptoethyl-carbamate linker in 15 might be slower than that of β-mercaptoisopropyl-carbamate linker in 14 (Zhang et al., 2018), which would allow sufficient time to form intramolecular disulfide 16.

The prodrug disulfide cleavage appeared to be operative in both human and rat blood. Further degradation of 11, 12, or 16 will release payload 2. In this context, linker disulfide cleavage could be a minor pathway in human blood and more cleavage in rat blood. ADC 13 primarily underwent prodrug disulfide cleavage in both human and rat blood for formation of intramolecular disulfide 16. The antibody-related product profile also indicated mainly prodrug disulfide cleavage, leading to loss of 196 Da species for formation of P1–P4 (Fig. 3, B and D).

The disulfide stability data with these PBD monomer model compounds 3–6 and ADC 13 suggest that there may be an enzymatic mechanism that causes instability of these stable disulfides in the whole blood incubations. Figure 2 (Pathway B) shows a proposed catalytic mechanism that can catalyze the disulfide cleavage of some of these model's disulfide compounds that release PBD 1 or 2 after linker immolation.

There is a good level (nanomolar to micromolar) of TRX and GRX in the whole blood of humans and animals (Björnstedt et al., 1995; Butera et al., 2014; Pei et al., 2018), which may have caused the instability of these disulfide compounds. Therefore, we conducted experiments using recombinant TRX and GRX enzymes in incubations with these disulfide compounds. The result was that an appreciable level of PBD monomer 1 was produced from compound 3 in the presence of TRX, TRX-reductase, and NADPH. However, GRX did not form any PBD monomer 1 from 3 in the presence of GSH at a concentration (80 μM), which did not chemically cleave the disulfide bonds (Fig. 5A). Surprisingly, GRX formed a similar low level of PBD monomer 1 for compounds 5 and 10 (Supplemental Table 2), which have different disulfide structures from that in compound 3. These results suggested that GRX has different specificity and perhaps narrower range of substrate than TRX for catalytic cleavage of disulfide bonds.

We next investigated whether the linker disulfide in ADC 12 is subject to catalytic disulfide cleavage by TRX or GRX. Figure 5B (conditions *a*, *b*, and *c*) showed that incubations of ADC 12 with both human and rat TRX produced PBD dimer 2 after 1 to 2 hours of incubation. In comparison, there was a minimal level of PBD dimer 2 formed in the incubations of human TRX without NADPH or in the presence of a TRX-reductase inhibitor (Fig. 5B, conditions *g* and *h*). GRX only produced a lower level of PBD dimer 2 (3- to 4-fold lower than TRX incubations) (Fig. 5B, conditions *d*, *e*, and *f*). No PBD dimer 2 formed in the control incubation in the presence of 80 μM GSH cofactor without GRX. Therefore, the TRX-mediated cleavage of the linker disulfide appeared to be time- and NADPH-dependent and can be inhibited by an inhibitor for TRX reductase (Fig. 5B).

Figure 5C shows PBD-related product formation from incubation of ADC 13 with TRX or GRX under various conditions. Payload 2 was the main product in incubations with human and rat TRX (conditions *a*, *b*, and *c*), and this activity was absent with the TRX reductase inhibitor presence or no NADPH (conditions *g* and *h*). Prodrug 11 was also a prominent metabolite in the incubation of human and rat TRX (conditions *a–d*). The intramolecular disulfide 16 was a minor product of TRX and GRX. PBD 2 was identified from incubation with TRX in the presence of TRX-reductase and NADPH or GRX at a concentration of GSH that did not cause any level of disulfide linker cleavage (Fig. 5C).

Similar to whole blood incubations, linker disulfide cleavage led to formation of proposed intermediate 14, which could quickly immolate to form prodrug 11. The disulfide in prodrug 11 can be further cleaved to form payload 2. Alternatively, disulfide cleavage in the prodrug functionality produced intermediate 15, which underwent relatively slower immolation that allowed for the formation of intramolecular disulfide 16. Supplemental Figure 2 shows the antibody-related product profiles of ADC 12 and 13 in the presence of human or rat TRX as well as human GRX. Compared with those profiles in whole blood (Fig. 3, B and D), the conjugate was more extensively degraded in the incubation with TRX, as evidenced by the formation of antibody that resulted from complete linker cleavage, which was not observed in whole blood incubations. Either prodrug disulfide or linker disulfide in ADC 13 could be cleaved by TRX or GRX to form a mix of products (Fig. 5C). GRX shows a low level of catalytic activity for both types of disulfide bonds.

The linker disulfide bond in ADC 12 was also cleaved by TRX, but the extent of the cleavage was much less than that in ADC 13 because there was still a significant amount of starting ADC 12 left in the parallel incubations (Supplemental Fig. 2, conditions *b* and *d*). Comparison of the antibody-related product profiles of ADC 12 and ADC 13 in the presence of TRX clearly showed that there was more extensive degradation of ADC 13 than 12 (Supplemental Fig. 2). Overall, the prodrug disulfide is more susceptible to catalytic cleavage by enzymes than the linker disulfide.

Discussion

Incubations of the disulfide-containing prodrugs 3, 5, and 10 with recombinant TRX and GRX in the presence of cofactors demonstrated catalytic activity to cleave the disulfide bonds in these small molecules. Incubation of ADC 12 with TRX and GRX also demonstrated their catalytic activities to cleave the linker disulfide. Incubation of ADC 13 further demonstrated that TRX and GRX can catalyze cleavage of both prodrug disulfide and linker disulfide bonds from the same molecule. These data clearly support the catalytic disulfide cleavage activities of TRX and GRX.

Both antibody product or PBD product profiles were qualitatively similar between the reactions of disulfide compounds used with TRX or GRX enzymes and whole blood. Immolation after disulfide cleavage for the disulfide-containing compounds selected in these studies facilitated the product analysis and clean assessment of disulfide cleavage. The disulfide linker cleavage in ADC 12 and 13 suggested accessibility of these disulfide bonds connecting the engineered-in cysteines and payloads. The variable stabilities of the ADC conjugates from the cysteines engineered at different locations on an antibody may suggest different accessibility of these linker disulfide bonds to TRX or GRX enzymes (Ohri, et al., 2018). Neither one of these enzymes is expected to cleave inner disulfide bonds such as the interchain disulfides of an antibody.

Cellular disulfide cleavage has been implied in a number of previous reports for cell incubations (Butera et al., 2014; Zhang et al., 2017a). TRX has been claimed to catalyze the allosteric disulfide bonds in proteins (Hogg, 2003, 2009). To our knowledge, there is no prior report of experimental data showing catalytic cleavage of disulfide bonds in xenobiotics by a particular enzyme. Disulfide-containing drugs are rare, so they may receive limited investigation in catalytic disulfide cleavage. Romidepsin, a disulfide-containing histone deacetylase inhibitor prodrug, is an anticancer agent used to treat cutaneous T-cell lymphoma (Amengual et al., 2018), and it binds to the thiol in the binding pocket of Zn-dependent histone deacetylase upon disulfide cleavage. TRX and GRX could also be involved in the metabolism of thiol-containing drugs such as albitiazolium (Caldarelli et al., 2012).

Collectively, our results support that TRX and GRX in whole blood may catalyze degradation of disulfide-containing prodrugs and disulfide-linker ADC conjugates. Through careful product characterization of probe disulfide-containing molecules, we have demonstrated that TRX and GRX catalyze the disulfide bond cleavage in xenobiotics, which represents a new function of TRX and GRX.

Acknowledgments

We would like to thank Hans Erickson and Becca Rowntree for discussion and support.

Authorship Contributions

Participated in research design: Zhang, Khojasteh.

Conducted experiments: Zhang, Fourie-O'Donohue, Dragovich, Pillow, Sadowsky, Kozak, Cass, L. Liu, Deng, Y. Liu.

Contributed new reagents or analytic tools: Zhang, Dragovich, Pillow, Sadowsky.

Performed data analysis: Zhang, L. Liu, Deng, Y. Liu, Khojasteh.

Wrote or contributed to the writing of the manuscript: Zhang, Fourie-O'Donohue, Dragovich, Pillow, Sadowsky, Kozak, Cass, L. Liu, Deng, Y. Liu, Hop, Khojasteh.

References

Amengual JE, Lichtenstein R, Lue J, Sawas A, Deng C, Lichtenstein E, Khan K, Atkins L, Rada A, Kim HA, et al. (2018) A phase 1 study of romidepsin and pralatrexate reveals marked activity in relapsed and refractory T-cell lymphoma. *Blood* **131**:397–407.

Azimi I, Wong JW, and Hogg PJ (2011) Control of mature protein function by allosteric disulfide bonds. *Antioxid Redox Signal* **14**:113–126.

Bhakta S, Raab H, and Junutula JR (2013) Engineering THIOMABs for site-specific conjugation of thiol-reactive linkers. *Methods Mol Biol* **1045**:189–203.

Björnstedt M, Hamberg M, Kumar S, Xue J, and Holmgren A (1995) Human thioredoxin reductase directly reduces lipid hydroperoxides by NADPH and selenocystine strongly stimulates the reaction via catalytically generated selenols. *J Biol Chem* **270**:11761–11764.

Butera D, Cook KM, Chiu J, Wong JW, and Hogg PJ (2014) Control of blood proteins by functional disulfide bonds. *Blood* **123**:2000–2007.

Caldarelli SA, Hamel M, Duckert JF, Ouattara M, Calas M, Maynadier M, Wein S, Périgaud C, Pellet A, Vial HJ, et al. (2012) Disulfide prodrugs of albitiazolium (T3/SAR97276): synthesis and biological activities. *J Med Chem* **55**:4619–4628.

Chen VM and Hogg PJ (2006) Allosteric disulfide bonds in thrombosis and thrombolysis. *J Thromb Haemost* **4**:2533–2541.

Chen Y and Hu L (2009) Design of anticancer prodrugs for reductive activation. *Med Res Rev* **29**: 29–64.

Erickson HK, Widdison WC, Mayo MF, Whiteman K, Audette C, Wilhelm SD, and Singh R (2010) Tumor delivery and in vivo processing of disulfide-linked and thioether-linked antibody-maytansinoid conjugates. *Bioconjug Chem* **21**:84–92.

Gamcsik MP, Kasibhatla MS, Teeter SD, and Colvin OM (2012) Glutathione levels in human tumors. *Biomarkers* **17**:671–691.

Hartley JA (2011) The development of pyrrolobenzodiazepines as antitumour agents. *Expert Opin Investig Drugs* **20**:733–744.

Hatem E, El Banna N, and Huang ME (2017) Multifaceted roles of glutathione and glutathione-based systems in carcinogenesis and anticancer drug resistance. *Antioxid Redox Signal* **27**: 1217–1234.

Hogg PJ (2003) Disulfide bonds as switches for protein function. *Trends Biochem Sci* **28**:210–214.

Hogg PJ (2009) Contribution of allosteric disulfide bonds to regulation of hemostasis. *J Thromb Haemost* **7** (Suppl 1):13–16.

Holmgren A and Björnstedt M (1995) Thioredoxin and thioredoxin reductase. *Methods Enzymol* **252**:199–208.

Jeffrey SC, Burke PJ, Lyon RP, Meyer DW, Sussman D, Anderson M, Hunter JH, Leiske CI, Miyamoto JB, Nicholas ND, et al. (2013) A potent anti-CD70 antibody-drug conjugate combining a

dimeric pyrrolobenzodiazepine drug with site-specific conjugation technology. *Bioconjug Chem* **24**: 1256–1263.
Johnson JM, Strobel FH, Reed M, Pohl J, and Jones DP (2008) A rapid LC-FTMS method for the analysis of cysteine, cystine and cysteine/cystine steady-state redox potential in human plasma. *Clin Chim Acta* **396**:43–48.
Junutula JR and Gerber HP (2016) Next-generation antibody-drug conjugates (ADCs) for cancer therapy. *ACS Med Chem Lett* **7**:972–973.
Kellogg BA, Garrett L, Kovtun Y, Lai KC, Leece B, Miller M, Payne G, Steeves R, Whiteman KR, Widdison W, et al. (2011) Disulfide-linked antibody-maytansinoid conjugates: optimization of in vivo activity by varying the steric hindrance at carbon atoms adjacent to the disulfide linkage. *Bioconjug Chem* **22**:717–727.
Lee MH, Yang Z, Lim CW, Lee YH, Dongbang S, Kang C, and Kim JS (2013) Disulfide-cleavage-triggered chemosensors and their biological applications. *Chem Rev* **113**:5071–5109.
Mustacich D and Powis G (2000) Thioredoxin reductase. *Biochem J* **346**:1–8.
Ohri R, Bhakta S, Fourie-O'Donohue A, Dela Cruz-Chuh J, Tsai SP, Cook R, Wei B, Ng C, Wong AW, Bos AB, et al. (2018) High-throughput cysteine scanning to identify stable antibody conjugation sites for maleimide- and disulfide-based linkers. *Bioconjug Chem* **29**:473–485.
Otani L, Ogawa S, Zhao Z, Nakazawa K, Umehara S, Yoshimura E, Chang SJ, and Kato H (2011) Optimized method for determining free L-cysteine in rat plasma by high-performance liquid chromatography with the 4-aminosulfonyl-7-fluoro-2,1,3-benzoxadiazole conversion reagent. *Biosci Biotechnol Biochem* **75**:2119–2124.
Pei Z, Chen C, Chen J, Cruz-Chuh JD, Delarosa R, Deng Y, Fourie-O'Donohue A, Figueroa I, Guo J, Jin W, et al. (2018) Exploration of pyrrolobenzodiazepine (PBD)-dimers containing disulfide-based prodrugs as payloads for antibody-drug conjugates. *Mol Pharm* **15**: 3979–3996.
Pillow TH, Sadowsky JD, Zhang D, Yu SF, Del Rosario G, Xu K, He J, Bhakta S, Ohri R, Kozak KR, et al. (2017a) Decoupling stability and release in disulfide bonds with antibody-small molecule conjugates. *Chem Sci (Camb)* **8**:366–370.
Pillow TH, Schutten M, Yu SF, Ohri R, Sadowsky J, Poon KA, Solis W, Zhong F, Del Rosario G, Go MAT, et al. (2017b) Modulating therapeutic activity and toxicity of pyrrolobenzodiazepine antibody-drug conjugates with self-immolative disulfide linkers. *Mol Cancer Ther* **16**:871–878.
Sato H, Shiiya A, Kimata M, Maebara K, Tamba M, Sakakura Y, Makino N, Sugiyama F, Yagami K, Moriguchi T, et al. (2005) Redox imbalance in cystine/glutamate transporter-deficient mice. *J Biol Chem* **280**:37423–37429.
Saunders LR, Bankovich AJ, Anderson WC, Aujay MA, Bheddah S, Black K, Desai R, Escarpe PA, Hampl J, Laysang A, et al. (2015) A DLL3-targeted antibody-drug conjugate eradicates high-grade pulmonary neuroendocrine tumor-initiating cells in vivo. *Sci Transl Med* **7**:302ra136.
Staben LR, Koenig SG, Lehar SM, Vandlen R, Zhang D, Chuh J, Yu SF, Ng C, Guo J, Liu Y, et al. (2016) Targeted drug delivery through the traceless release of tertiary and heteroaryl amines from antibody-drug conjugates. *Nat Chem* **8**:1112–1119.
Su D, Ng C, Khosraviani M, Yu S, Cosino E, Kaur S, and Xu K (2016) Custom-Designed Affinity Capture LC-MS F(ab')2 Assay for Bio-transformation Assessment of Site-Specific Antibody Drug Conjugates. *Analytical Chemistry* **88**(23):11340–11346.
Vrudhula VM, MacMaster JF, Li Z, Kerr DE, and Senter PD (2002) Reductively activated disulfide prodrugs of paclitaxel. *Bioorg Med Chem Lett* **12**:3591–3594.
Wang Y, Liu D, Zheng Q, Zhao Q, Zhang H, Ma Y, Fallon JK, Fu Q, Haynes MT, Lin G, et al. (2014) Disulfide bond bridge insertion turns hydrophobic anticancer prodrugs into self-assembled nanomedicines. *Nano Lett* **14**:5577–5583.
Zhang D, Pillow TH, Ma Y, Cruz-Chuh JD, Kozak KR, Sadowsky JD, Lewis Phillips GD, Guo J, Darwish M, Fan P, et al. (2016) Linker immolation determines cell killing activity of disulfide-linked pyrrolobenzodiazepine antibody-drug conjugates. *ACS Med Chem Lett* **7**:988–993.
Zhang D, Yu SF, Khojasteh SC, Ma Y, Pillow TH, Sadowsky JD, Su D, Kozak KR, Xu K, Polson AG, et al. (2018) Intratumoral payload concentration correlates with the activity of antibody-drug conjugates. *Mol Cancer Ther* **17**:677–685.
Zhang S, Guan J, Sun M, Zhang D, Zhang H, Sun B, Guo W, Lin B, Wang Y, He Z, et al. (2017a) Self-delivering prodrug-nanoassemblies fabricated by disulfide bond bridged oleate prodrug of docetaxel for breast cancer therapy. *Drug Deliv* **24**:1460–1469.
Zhang X, Li X, You Q, and Zhang X (2017b) Prodrug strategy for cancer cell-specific targeting: a recent overview. *Eur J Med Chem* **139**:542–563.

Address correspondence to: Dr. Donglu Zhang, Drug Metabolism & Pharmacokinetics, Genentech, Inc., 1 DNA Way MS 412a, South San Francisco, CA 94080. E-mail: zhang.donglu@gene.com; or Dr. S. Cyrus Khojasteh, Drug Metabolism & Pharmacokinetics, Genentech, Inc., 1 DNA Way MS 412a, South San Francisco, CA 94080. E-mail: khojasteh.cyrus@gene.com

Supplement Information

Catalytic cleavage of disulfide bonds in small molecules and linkers of antibody-drug conjugates

Donglu Zhang[1]*, Aimee Fourie-O'Donohue[2], Peter S Dragovich[3], Thomas H Pillow[3], Jack D Sadowsky[4], Katherine R Kozak[2], Robert T Cass[1], Liling Liu[1], Yuzhong Deng[1], Yichin Liu[2], Cornelis ECA Hop[1], S Cyrus Khojasteh[1]*

Affiliations:

Authors Affiliations:

Drug Metabolism & Pharmacokinetics (DZ, RTC, LL, YD, CECAH, SCK), Biochemical and Cellular Pharmacology (AFO, KRK, YL), Discovery Chemistry (PSD, THP), Protein Chemistry (JDS), Genentech, Inc., South San Francisco, CA 94080, USA.

*Correspondence to: zhang.donglu@gene.com

Table 1S. Concentrations of thiol species (GSH, GSSG, cysteine, cysteine) in plasma, whole blood, and blood cells of human and rat

		GSH (µM)	GSSG (µM)	Cysteine (µM)	Cystine (µM)
Human	Plasma	5.8 ± 0.6	<2.4	<2.4	26.1 ± 3.2
	Blood	284 ± 9	234 ± 25	<2.4	20.6 ± 4.0
	Blood cells	855 ± 50	315 ± 42	<2.4	11.9 ± 5.0
Rat	Plasma	7.8 ± 0.9	13.7 ± 1.1	<2.4	29.8 ± 1.3
	Blood	518 ± 26	92.0 ± 5.9	<2.4	23.7 ± 1.5
	Blood cells	1450 ± 64	160 ±8	29.4 ± 6.9	12.9 ± 3.0

The samples were treated with 5 volumes of 0.5 N perchloric acid with vortex and sonication for 5 min. The samples were analyzed by LC/MS/MS.

N=4, LLOQ = 1 µM (GSH), 2.4 µM (cysteine), 2.4 µM (GSSG), and 0.4 µM (cystine).

Table S2. Product formation of disulfide-containing prodrugs and ADC conjugates in incubation with TRX and GRX under various conditions

Reaction/ Condition	Cofactor	**Parent→**	**3**	**5**	**10**	**12**	**13**		
		Product→	**1**	**1**	**1**	**2**	**2**	**16**	**11**
+hTRX 2h	+NADPH		++	+	+	++	++	+	++
+hTRX 1h	+NADPH		ND	ND	ND	++	++	-	++
+rTRX 1h	+NADPH		ND	ND	ND	++	++	+	++
+hGRX 2h	+GSH		-	+	+	+	+	+	++
+hGRX 1h	+GSH		ND	ND	ND	+	-	+	+
+hGRX 2h	-GSH		ND	ND	ND	+	-	-	-
+hTRX+inhibitor 2h	+NADPH		ND	ND	ND	-	-	-	-
+hTRX 2h	-NADPH		-	-	-	-	-	-	-
-hTRX 2h	+NADPH		ND	ND	ND	-	-	-	-
-hGRX	+GSH		-	-	-	-	-	-	-

Note: ++, +, -, and ND shows decreasing amounts.

Figure 1S. Stability of disulfide-containing prodrugs in human and rat blood incubations

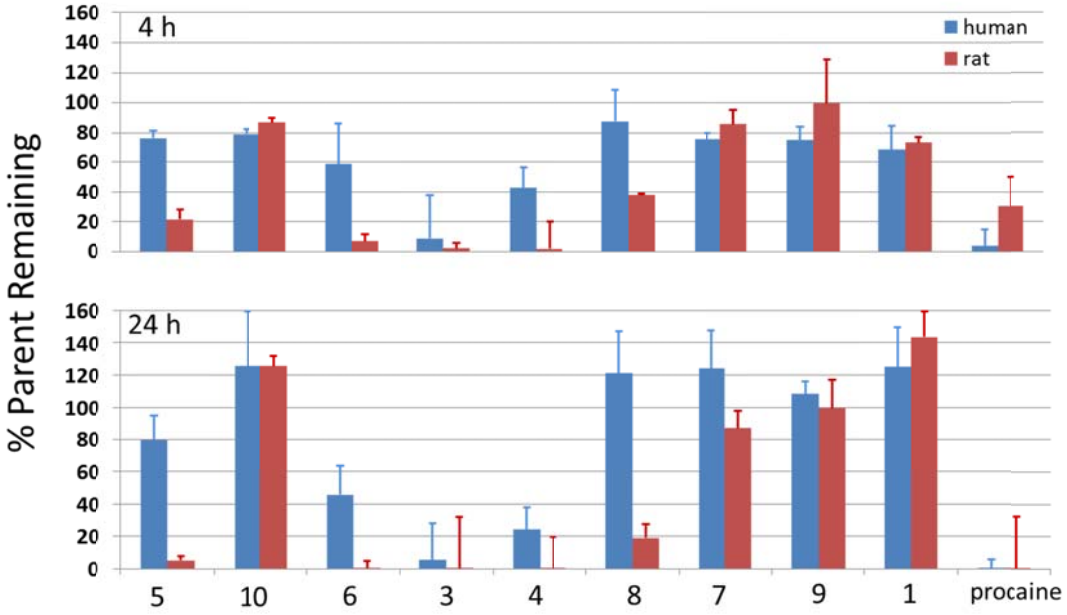

Figure 2S. Antibody-related product profiles of ADC **12** and **13** in incubations with TRX and GRX.

ADC12 = Ab + 2*LD; P-2 = Ab + LD

ADC13 = Ab + 2*LD; P-3=Ab+LD-196Da; P1=Ab+LD+CYS-196Da;

P3=Ab+2*LD-2*196Da; P4=Ab+2*LD-196Da

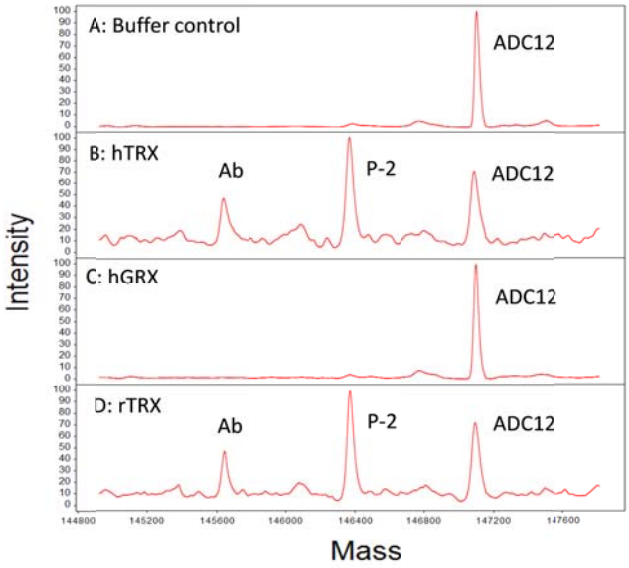

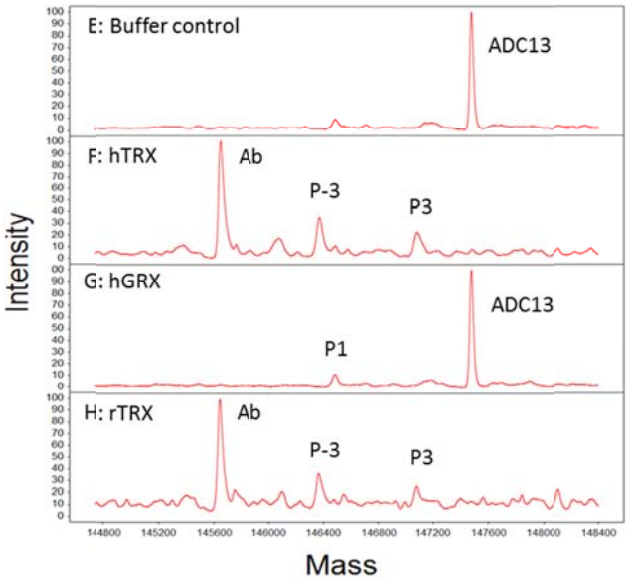

Synthesis of compounds

Compound 11

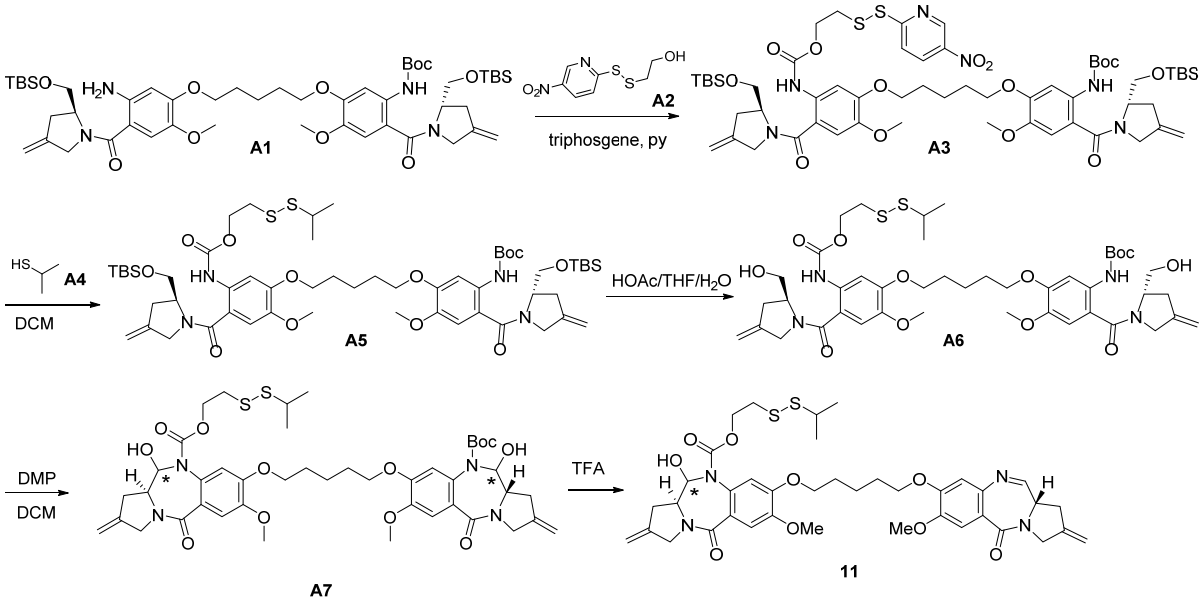

To a solution of triphosgene (89.43 mg, 0.300 mmol) and 4Å molecular sieves (50 mg) in DCM (5.0 mL) was added a solution of compound **A2** (165.0 mg, 0.710 mmol) and pyridine (168.58 mg, 2.13 mmol) in dichloromethane (DCM) (5.0 mL). The mixture was stirred at 0 °C for 30 min. The resulting mixture was added dropwise to a solution of compound **A1** (745 mg, 0.780 mmol), pyridine (169 mg, 2.13 mmol) and 4Å MS in DCM (5.0 mL). It was stirred at 0 °C for 30 min, and washed with water (5.0 mL). The organic phase was dried, concentrated and purified by flash column chromatography (5% MeOH in DCM) to give the product **A3** (698 mg, 81%) as a yellow oil. LC/MS (5-95, AB, 1.5 min): RT =1.187 min, m/z=606.5 [M/2+1]+.

To a solution of compound **A3** (698.0 mg, 0.580 mmol) in DCM (10.0 mL) was added 2-propanethiol (439 mg, 5.76 mmol). After the mixture was stirred at 20 °C for 1

h, MnO_2 (100 mg) was added and stirred for 5 min, and filtered. The filtrate was concentrated and purified by prep-TLC (50% EtOAc in petroleum ether) to give compound **A5** (620 mg, 95%) as a yellow solid. LC/MS (5-95, AB, 1.5 min): RT =1.221 min, m/z=1131.4 [M+1]+.

To a solution of compound **A5** (620.0 mg, 0.550 mmol) in THF (6.0 mL) and water (6.0 mL) was added HOAc (3.29 g, 54.8 mmol). The mixture was stirred at 40 °C for 16 h and concentrated. It was purified by column chromatography (10% MeOH in DCM) to afford compound **A6** (208 mg, 42%) as yellow oil. LCMS (5-95, AB, 1.5 min): RT = 0.854 min, m/z=903.3 [M+1]+.

To a solution of compound **A6** (208.0 mg, 0.230 mmol) in DCM (8.0 mL) was added 4Å molecular sieves, DMP (224.7 mg, 0.530 mmol). The mixture was stirred at 20 °C for 2 h and was quenched with saturated $NaHCO_3$ and $Na_2S_2O_3$ solution (2.0 mL/2.0 mL). After it was stirred for 5 min, DCM (5.0 mL) was added and separated. The DCM phase was washed with water (2 x 5 mL). It was dried, concentrated and purified by prep-TLC (5% MeOH in DCM, Rf=0.2) to afford compound **A7** (121 mg, 58%) as a light yellow foam. LC/MS (5-95, AB, 1.5 min): RT =0.783 min, m/z=781.3 [M-100+1]+.

TFA (1.0 mL, 13.5 mmol) was added to compound **A7** (121.0 mg, 0.130 mmol) at 0 °C. After the mixture was stirred for 10 min, it was added to a cold saturated $NaHCO_3$ solution (20 mL) and extracted with DCM (3 x 10 mL). The combined organic layers were concentrated and purified by prep-TLC (10% MeOH in DCM, Rf = 0.2) followed by prep-HPLC (ACN, acetonitrile: 42~62%, 0.225%FA) to afford the title compound **11** (7.2 mg, 7.0%). LC/MS (5-95, AB, 1.5 min): RT =0.868 min, m/z=781.3 [M+1]+.

Compound B8

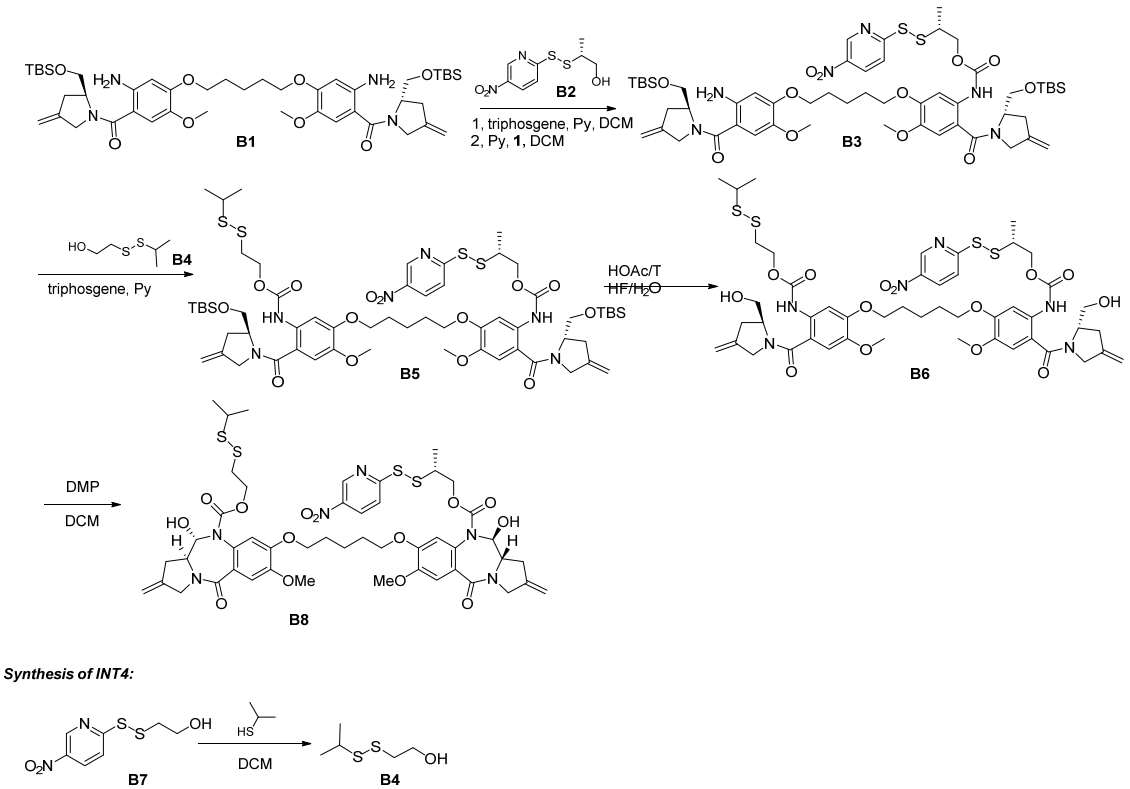

To a mixture of compound **B7** (200 mg, 0.86 mmol) in DCM (10 mL) was added 2-propanethiol (328 mg, 4.31 mmol). The mixture was stirred at 15 °C for 12 h. The solid was filtered and the solution was concentrated. The residue was purified by chromatography on silica (100% DCM) to give compound **B4** (90 mg, 69%) as a colorless oil. ^{1}HNMR (400 MHz, $CDCl_3$) δ 3.91-3.86 (m, 2 H), 3.05-3.00 (m, 1H), 2.86-2.84 (m, 2H), 2.04 (t, J = 6.4 Hz, 1H), 1.32 (d, J = 6.4 Hz, 1H).

To a solution of triphosgene (301 mg, 1.01 mmol) in DCM (5.0 mL) was added a mixture of compound B**2** (500 mg, 2.03 mmol) and pyridine (161 mg, 2.03 mmol) in DCM (5.0 mL) at 0 °C under N_2. The reaction mixture was stirred at 16 °C for 30 min. The mixture was concentrated in vacuo and used in the next step directly. To a solution

of the above mixture in DCM (5.0 mL) was added a mixture of compound B**1** (2.76 g, 3.24 mmol) and pyridine (128 mg, 1.62 mmol) in DCM (45.0 mL) at 0 °C. The reaction mixture was stirred at 0 °C for 1 h. TLC (50% EtOAc in petroleum ether Rf = 0.6) showed that the product B**3** was formed. The reaction mixture was concentrated in vacuo and purified by chromatography on silica (0-50% EtOAc in petroleum ether) to give compound B**3** (1.50 g, 78.2%) as a yellow solid. LC/MS (5-95, AB, 1.5 min): R_T = 1.09 min, *m/z* = 1126.7 $[M+1]^+$.

To a mixture of compound **B3** (200 mg, 0.18 mmol) and Et_3N (36 mg, 0.36 mmol) in DCM (4.0 mL) was added triphosgene (26 mg, 0.09 mmol) in DCM (2.0 mL) at 0 °C. After addition, the mixture was stirred at 15 °C for 20 min. LCMS (sample quenched with MeOH, 5-95, AB, 1.5 min): R_T = 1.164 min, *m/z* = 1183.4 $[M+32+1]^+$. The mixture was used directly in the next step. To above mixture was added a solution of compound **B4** (38 mg, 0.25 mmol) and Et_3N (34 mg, 0.33 mmol) in DCM (1.0 mL). After the reaction mixture was stirred at 15 °C for 2 h, it was concentrated and purified by prep-TLC (33% EtOAc in petroleum ether, Rf=0.4) to give compound **B5** (160 mg, 72%) as a yellow oil. LC/MS (5-95, AB, 1.5 min): R_T = 1.26 min, *m/z* = 1304.2 $[M+1]^+$.

To a mixture of compound **B5** (160 mg, 0.12 mmol) in THF (2.0 mL) and water (2.0 mL) was added HOAc (3.91 mL, 68 mmol) dropwise. After addition, the mixture was stirred at 15 °C for 12 h. TLC (5% MeOH in DCM, Rf = 0.5) showed was complete. The mixture was poured into EtOAc (30 mL), and was washed with water (10 mL x 2), saturated $NaHCO_3$ (10 mL x 2) and brine (10 mL). The organic layer was dried over Na_2SO_4 and purified by prep-TLC (5% MeOH in DCM, Rf = 0.5) to give compound **B6**

(120 mg, 93%) as a yellow solid. LC/MS (5-95, AB, 1.5 min): R_T = 0.88 min, *m/z* = 1075.5 $[M+1]^+$.

To a mixture of compound **B6** (60 mg, 0.06 mmol) in DCM (5.0 mL) was added DMP (71 mg, 0.17 mmol). The reaction mixture was stirred at 15 °C for 1 h. LCMS (5-95AB/1.5min): RT =0.80 min, $[M+H]^+$1071.2 showed 39% of desired product. The mixture was concentrated and the residue was purified by prep-TLC (7% MeOH in DCM, Rf = 0.5), followed by prep-HPLC (acetonitrile 45-75/10mM NH_4HCO_3-ACN) to give **B8** (10.1 mg, 17%) as a white solid. LC/MS (5-95, AB, 1.5 min): R_T = 0.81 min, *m/z* = 1053.1 $[M-18+1]^+$. ^{1}H NMR (400 MHz, $CDCl_3$) δ 9.22 (s, 1H), 8.30 (d, *J* = 7.6 Hz, 1H), 7.63 (d, *J* = 8.8 Hz, 1H), 7.27 (s, 1H), 7.21 (s, 1H), 6.86 (s, 1H), 6.70 (s, 1H), 5.59-5.56 (m, 2H), 5.15 (s, 4H), 4.43-4.29 (m, 4H), 4.17-3.64 (m, 19 H), 3.22-3.20 (m, 1H), 2.94-2.70 (m, 6H), 1.91 (d, *J* = 6.4 Hz, 4H), 1.64 (s, 2H), 1.26-1.20 (m, 9H).